

PCCP

Accepted Manuscript



This is an *Accepted Manuscript*, which has been through the Royal Society of Chemistry peer review process and has been accepted for publication.

Accepted Manuscripts are published online shortly after acceptance, before technical editing, formatting and proof reading. Using this free service, authors can make their results available to the community, in citable form, before we publish the edited article. We will replace this *Accepted Manuscript* with the edited and formatted *Advance Article* as soon as it is available.

You can find more information about *Accepted Manuscripts* in the [Information for Authors](#).

Please note that technical editing may introduce minor changes to the text and/or graphics, which may alter content. The journal's standard [Terms & Conditions](#) and the [Ethical guidelines](#) still apply. In no event shall the Royal Society of Chemistry be held responsible for any errors or omissions in this *Accepted Manuscript* or any consequences arising from the use of any information it contains.



PCCP

ARTICLE

An advanced approach for measuring acidity of hydroxyls in confined space: FTIR study of low-temperature CO and $^{15}\text{N}_2$ adsorption on MOF samples from the MIL-53(Al) series

Received 00th January 20xx,
Accepted 00th January 20xx

DOI: 10.1039/x0xx00000x

www.rsc.org/

M. Mihaylov,^a S. Andonova,^a K. Chakarova,^a A. Vimont,^b E. Ivanova,^a N. Drenchev^a and K. Hadjiivanov^{a,*}

Acidity of solids is decisive for their interaction with guest molecules. One of the most used ways for measuring the acidity of surface hydroxyl groups is the hydrogen bond method based on the spectral shift of the OH stretching modes induced by adsorption of weak bases. However, many materials of practical interest (e.g. metal organic frameworks, zeolites, etc.) are porous and the OH groups are involved in H-bonding with framework basic sites. Here we show that MIL-53(Al) and NH_2 -MIL-53(Al) samples are characterized by one type of structural hydroxyls but three IR bands are detected at 100 K with these materials (at 3721, 3711 and 3683 cm^{-1}). These bands are assigned to structural hydroxyls involved in H-bonding with different strength. There is no correlation between the acidities of the hydroxyls, as measured by low-temperature CO or $^{15}\text{N}_2$ adsorption, and the main reason for this is the pre-existing H-bond. A method for estimation of the intrinsic frequency of the OH groups (i.e. if not participating in H-bonds), based on analysis of the spectral data obtained with two molecular probes, is proposed. According to this method, the OH stretching frequency of the structural hydroxyls of MIL-53(Al) samples is determined to be 3727 cm^{-1} . Formation of 1 : 1 adducts between the hydroxyls and strong bases leads to breaking of the pre-existing H-bonds. When the base is weak, bifurcated complexes are formed which slightly affects the spectral shift. The conclusions derived here considerably broaden the applicability of the H-bond method for assessing protonic acidity to materials and systems where the OH groups are preliminary involved in H-bonding.

Introduction

Surface Brønsted acidity of different materials is decisive for their adsorption and catalytic properties.^{1–4} For that reason, thousands of investigations deal with the determination of acidity of particular surface hydroxyl groups. Among the different techniques, spectroscopic measurements are usually preferred because they give selective information on different hydroxyls. One of the approaches applied is the so-called ion-pair method based on the protonation of strong bases such as pyridine and ammonia.^{4–6} A drawback of this technique is that the process is strongly affected by the subsequent stabilization of the protonated molecule through bonding to one or more basic sites from the material. In addition, no direct spectral information on the strength of the acid sites can be obtained.

The most widely used technique is the so-called hydrogen-bond method.^{4–6} Upon formation of an H-bond between the H-atom from the hydroxyl group and a basic molecule, the O–H distance increases and the O–H bond order decreases. This

reflects in a shift of the $\nu(\text{OH})$ modes towards lower wavenumbers. Further consequences of the formation of an H-bond are (i) the increase in intensity and (ii) the broadening of the $\nu(\text{OH})$ bands. The intensity increase is caused by the elongation of the OH bond and the resulting increase of the hydroxyl dipole moment while the broadening arises from coupling of $\nu(\text{OH})$ with the hydrogen bond stretching vibration (via both sum and difference combinations). It was reported that the bathochromic shift of the $\nu(\text{OH})$ modes correlates with the acidity of the hydroxyls, which is the base of the H-bond method. Because the method gives direct quantitative values it has gained a big popularity.

In fact the hydrogen bond method measures the proton affinity (PA) of the hydroxyl group (i.e. the dissociation enthalpy) and the following equation is used for weak H-bonds:⁶

$$\text{PA}^{\text{OH}} = \text{PA}^{\text{SiOH}} - 442.5 \log (\Delta \tilde{\nu}(\text{OH}) / \Delta \tilde{\nu}(\text{SiOH})) \quad (1)$$

where PA^{OH} and PA^{SiOH} are the proton affinities (in kJ mol^{-1}) of the investigated OH groups and of silanol groups, respectively, and PA^{SiOH} is 1390 kJ mol^{-1} . An important conclusion is that PA^{OH} should be the same as measured by different bases.

Among the most used probe molecules for measuring protonic acidity are CO (PA at the C-atom of 594 kJ mol^{-1} ⁷) and N_2 (PA of 493.8 kJ mol^{-1} ⁷). Numerous data with benzene, alkanes, alkenes, H_2 and other adsorbates are also available.

^a Institute of General and Inorganic Chemistry, Bulgarian Academy of Sciences, Sofia 1113, Bulgaria

^b Laboratoire Catalyse et Spectrochimie, UMR CNRS 6506 – ENSICAEN, 6 Bd du Maréchal Juin, 14050 CAEN Cedex, France

† Electronic Supplementary Information (ESI) available: [Experimental details, and supporting FTIR spectra]. See DOI: 10.1039/x0xx00000x

However, it was recently emphasized⁴ that most of these molecules tend to be bonded, in addition to the proton from the hydroxyl group, to a basic site (usually O²⁻). This complicates the spectra and affects the precision of the acidity measurements. Therefore, here we will concentrate on the data obtained with CO and N₂ because these molecules are "on-top" adsorbed on OH groups.⁴

In most cases there is a good agreement between the PA of the hydroxyls measured by CO and N₂ molecular probes.^{4,8-11} Analysis of the literature data⁴ shows that the CO-induced shift of the silanol O-H modes is 2.8 times larger than the N₂-induced shift, in line with the higher basicity of CO. Moreover, similar values (ca. 2.7 ± 0.15) have been reported for various hydroxyl groups. However, there are some problems with the application of the hydrogen-bond method especially when studying porous materials. It is well known that the OH groups in microporous solids are involved in weak H-bonding with the framework.¹² As a result, the OH stretching modes are shifted to lower wavenumbers. It has already been pointed out^{13,14} that the acidity estimation based on the measured $\nu(\text{OH})$ value of OH groups that have been preliminary involved in H-bonding should not correspond to the true acidity of the hydroxyls.

Thus a question arises: which value of $\nu(\text{OH})$ should be used as a reference for determination of the spectral shift: the measured frequency or the frequency expected if the OH groups are not involved in any H-bonding? Jacobs and Mortier¹² proposed a frequency of 3645 cm⁻¹ for the "free" bridging Al-(OH)-Si groups in zeolites. However, due to the diversity of the OH groups in MOFs and in many other porous materials, no reference value can be proposed in these cases.

The problem with the reference $\nu(\text{OH})$ value is particularly very important when assessing the acidity of the so-called pseudo-bridging hydroxyls. A very high acidity of silanol groups on silica-alumina (ca. 3745 cm⁻¹) was measured by several research groups.¹⁵⁻¹⁸ This phenomenon has been rationalized by Busca et al.¹⁵ who proposed that upon complexation with basic molecules (e.g. CD₃CN) the SiOH groups change their configuration and are transformed into Si-(OH)-Al bridging hydroxyls. In this case the reference $\nu(\text{OH})$ value used is the frequency of the silanol groups, 3745 cm⁻¹. However, referring to the value proposed for bridging hydroxyls not involved in H-bonding (3645 cm⁻¹) will automatically decrease the absolute value of the shifts by 100 cm⁻¹ which corresponds to a lower acidity.

In this work we report the results of CO and N₂ adsorption on MOF samples from the MIL-53 series (MIL stands for Matériaux de l'Institut Lavoisier). These materials have provoked a big interest¹⁹⁻³¹ mainly due to their potential application for CO₂ capture. MIL-53(Al) is aluminum hydroxoterephthalate and is build up by infinite trans chains of corner-sharing, via OH groups, AlO₄(OH)₂ octahedra linked by 1,4-benzenedicarboxylate ligands.^{19,20,22,25,28} It has a three-dimensional skeleton structure with pores large up to 0.85 nm. A peculiarity of this material is that it is among the so-called breathing MOFs.^{20,28} At low-temperature MIL-53(Al) is in the large-pore form and upon heating is reversibly transformed

into the narrow-pore form. With the aim of developing more effective CO₂ adsorbents, NH₂-MIL-53(Al) MOF was synthesized.¹⁹ This material exhibits the same topology as MIL-53(Al) but in this case the linker is 2-amino terephthalate anion.^{19,20,25,28} Due to the H-bonding between the NH₂ and OH groups NH₂-MIL-53(Al) is in a narrow pore form.^{20,25}

The relatively weak acidity of the hydroxyl groups in these MOFs⁴ and the existence of well defined OH groups involved in H-bonding in NH₂-MIL-53(Al) allowed us to conclude on the importance of the (i) pre-existing H-bonds and (ii) formation of bifurcated complexes, as well as how these factors affect the correctness of the H-bond method for measuring the acidity of hydroxyls.

Experimental

The MIL-53(Al) sample was a commercial BASF product Basolite® A100. Two different activation temperatures were applied for this material, namely 473 and 623 K. The sample activated at 473 K contained residual terephthalic acid which was removed after evacuation at 623 K, as seen from the disappearance of the diagnostic IR band at 1699 cm⁻¹ (see Fig S1, spectra a and b from ESI). Hereafter, the sample activated at 473 K (200 °C) will be denoted as M-200, while the sample activated at 623 K (350 °C), as M-350.

The amino-functionalized sample, NH₂-MIL-53(Al), was provided by TU Delft and synthesis details are reported elsewhere.¹⁹ The sample was acid-free and was activated under vacuum at 473 K for 30 min.

Some characteristics of the samples and the notations that will be used further on are summarized in Table 1.

Table 1. Some details on the samples studied in this work.

Notation	Sample	Origin	Evacuated at:
M-200	MIL-53(Al)	BASF ^a	473 K
M-350	MIL-53(Al)	BASF ^a	623 K
NM	NH ₂ -MIL-53(Al)	TU Delft	473 K

^a The trade name is Basolite® A100.

The IR measurements were performed with Nicolet Avatar 360 and Nicolet 6700 FTIR spectrometers accumulating 64 scans at a spectral resolution of 2 cm⁻¹. A specially designed IR cell was used which allowed registering the spectra at low and ambient temperatures. The cell was connected to a vacuum-adsorption apparatus with a residual pressure lower than 10⁻³ Pa.

The IR spectra were obtained with self-supporting pellets and with samples spread onto KBr pellets. The results obtained were essentially the same. However, with the self-supporting pellets some bands were too intense and out of scale, which hindered the quantitative estimations. The presented spectra are recorded with KBr-spread materials except when specially noted.

Deuteration was performed with D₂O vapor (5 mbar pressure) at 473 K for 30 min followed by evacuation at the

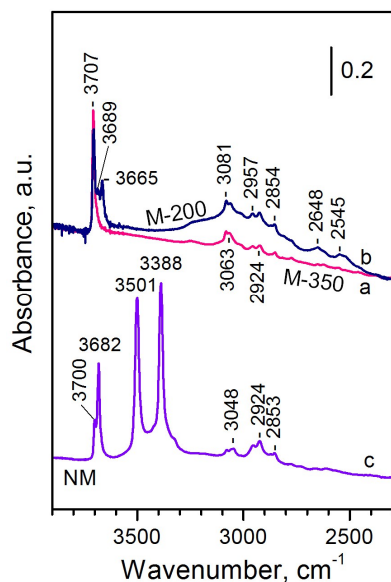


Fig. 1. Background spectra of the M-350 (a), M-200 (b) and NM samples (c).

same temperature. This procedure was repeated three times which resulted in ca. 75 % degree of deuteration.

To ensure isothermal conditions in the low-temperature adsorption experiments, the cell was first cooled down and filled in with He (50 mbar pressure). Then the desired amount of adsorbate was added to the system.

Carbon monoxide (>99.5% purity) was supplied by Merck. Labeled dinitrogen ($^{15}\text{N}_2$, isotopic purity of 99.7%) was provided by Isotec Inc. (a Matheson USA company). D_2O originated from Cambridge Isotope Laboratories, Inc. and had isotopic purity of 99.9%. Helium was supplied by Messer and had a purity of 99.999 %.

Results

Background spectra

The first main goal of this study is the precise assignment of the hydroxyl bands. The spectra of the MIL-53(Al) and NH_2 -MIL-53(Al) MOF compounds are already reported in the literature and here we will concentrate mainly on the OH stretching region. Some details for the other bands are provided in the ESI (see Fig. S1).

Sample M-350. According to the literature,^{21,22} MIL-53(Al) is characterized by structural μ_2 -OH species absorbing at 3708–3702 cm^{-1} . These bridging hydroxyls are located at the trans-corner sharing octahedra $\text{AlO}_4(\text{OH})_2$ chains. The spectrum of the acid-free M-350 sample (Figs. 1 and 2, spectra a) is generally consistent with these previous reports. A sharp band at 3707 cm^{-1} dominates in the OH region. Computer deconvolution (see Fig. S2 in the ESI) suggests that the band consists of two components, the lower-frequency component

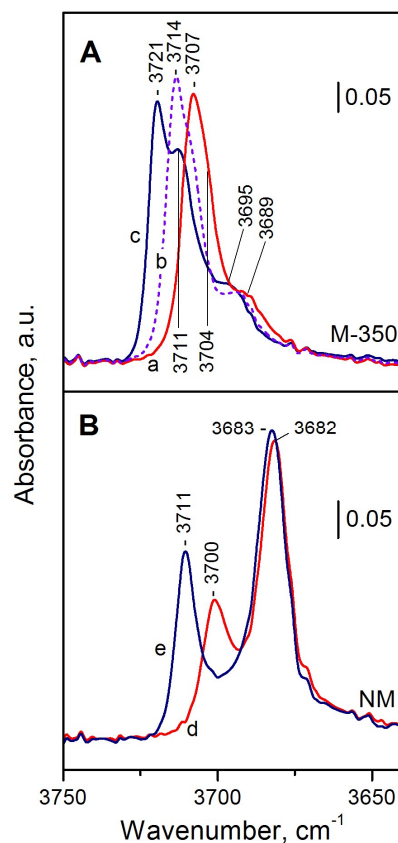


Fig. 2. Effect of temperature on the hydroxyl spectra of the MOF samples. Ambient temperature (a, d); ca. 100 K and in presence of 50 mbar He (c, e); and after evacuation of He at low temperature (b).

is slightly broader indicating a weak H-bonding. A low-intensity and broad shoulder at ca. 3689 cm^{-1} is also discernible. This shoulder characterizes some OH groups involved in H-bonding with small amounts of residual terephthalic acid.

Because the adsorption experiments were performed at low temperature, it is essential to know in details the temperature effect on the background spectra. Temperature hardly affects the spectra in the low-frequency region but has a strong effect on the spectra in the OH stretching region.

At 100 K and in presence of He the two components of the OH bands registered with the M-350 sample are shifted to higher frequencies (3721 and 3711 cm^{-1} , respectively) and become better resolved (Fig. 2A, spectrum c). The shoulder at 3689 cm^{-1} is also shifted, by ca. 6 cm^{-1} .

It was also established that the shift is gradual and its value decreases with evacuation of He at low temperature (Fig. 2A, spectrum b) and with subsequent heating up to ambient temperature. Note that the presence of He in the system leads to a decrease of the pellet temperature due to improved thermoconductivity. In any case, to eliminate the temperature effect when studying low-temperature CO and N_2 adsorption,

the adsorbates were introduced after preliminary introduction of He to the sample.

The spectra of the M-350 sample in the low-frequency region are discussed in the ESI (see Section 2 and Fig. S1A).²²⁻²⁴ In particular, a very intense $\delta(\text{OH})$ band is detected around 984 cm^{-1} at low temperature. However, the high intensity of the band does not allow exact maximum determination and analysis of eventual band components.

Sample M-200. When the MIL-53(Al) sample was activated only at 473 K, it contained residual terephthalic acid²⁵ (for details see Section 1 in the ESI). The hydroxyl IR spectrum in this case is more complicated (Fig. 1, spectrum b). The principal OH band was detected at 3705 cm^{-1} . Another OH band, at 3665 cm^{-1} , was also registered. At lower wavenumbers a broad band centred around 3000 cm^{-1} can also be distinguished and is assigned to OH groups from the residual acid involved in H-bonding with the MOF framework. Two other weak bands at 2648 and 2545 cm^{-1} are typical of facing and H-bonded COOH groups from the acid.³² Additional experiments showed that increase of the evacuation temperature results in decrease of the amount of residual acid and successive disappearance of the bands at 3665 and 3689 cm^{-1} . This suggests that these two bands are due to the MOF structural hydroxyls involved in H-bonding with the residual acid.

The hydroxyl spectra of the M-200 and M-350 samples registered at low temperature are compared in Fig. 3A. In particular, it is evident that the low frequency component at 3711 cm^{-1} appears with strongly enhanced intensity with the M-200 sample at the expense of the component at 3721 cm^{-1} .

Fig. 3B shows the $1050 - 1000\text{ cm}^{-1}$ region where the C-H deformation (ν_{18a}) modes of the terephthalate ligands are observed. The position of this band is indicative of the large pore (1024 cm^{-1}) and narrow pore (1019 cm^{-1}) forms of the MOF structure.²² A good correlation between the intensities of the bands at 3721 and 1024 cm^{-1} , on one hand, and the bands at 3711 and 1019 cm^{-1} , on the other hand, is evident. These results strongly suggest that the band at 3721 cm^{-1} is associated with the large (open) pore MOF structure and the band at 3711 cm^{-1} , with the narrow (closed) pore form. Additional proofs of this assignment are: (i) the 3711 cm^{-1} band is broader (FWHM of 8 cm^{-1}) than the band at 3721 cm^{-1} (FWHM of 5 cm^{-1}) which indicates some H-bonding favoured by the pore narrowing; (ii) the band at 3721 cm^{-1} was not observed with the narrow-pore NM sample (vide infra); and (iii) there is only one kind of structural hydroxyl groups in the MIL-53(Al) materials.

Sample NM. Consider now the amino-functionalized sample (Fig. 1, spectrum c). Its spectrum is also in agreement with the published data for this material.^{19,20,23,25-30} In particular, two intense bands at 3501 and 3388 cm^{-1} characterize the symmetric and antisymmetric N-H modes of the amino groups.^{19,23,28} In the hydroxyl stretching region two $\nu(\text{OH})$ bands, at 3700 and 3682 cm^{-1} , are observed. The band at 3700 cm^{-1} is assigned to structural $\mu_2\text{-OH}$ groups also typical of the amino-free MIL-53(Al) sample. The lower frequency band, at 3682 cm^{-1} , is attributed to a fraction of the structural

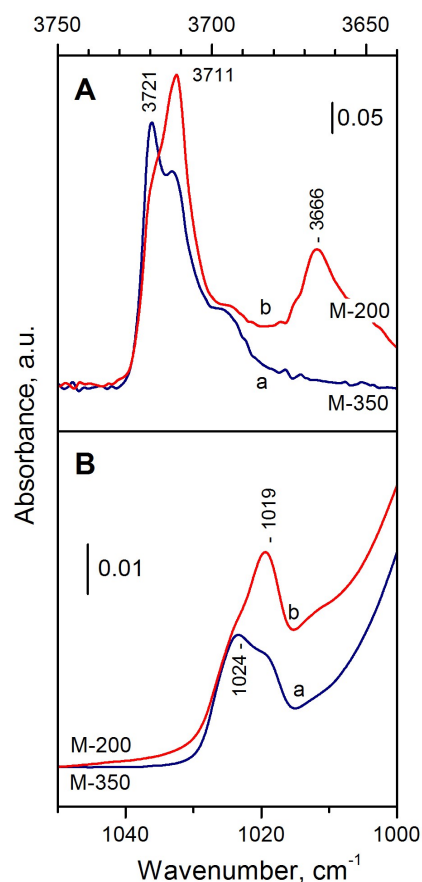


Fig. 3 FTIR spectra of M-350 (a) and M-200 (b) registered at 100 K and in presence of 50 mbar He.

OH groups involved in H-bonding with the amino groups.^{19,23,28} In agreement with this assignment, the FWHM of the 3682 cm^{-1} band is 11.4 cm^{-1} vs. 8.6 cm^{-1} for the band at 3700 cm^{-1} .

Fig. 2B shows the effect of temperature on the hydroxyl spectra of the NM sample. Lowering the temperature to ca. 100 K (in presence of He) leads to blue shift of the hydroxyl bands, to 3711 and 3683 cm^{-1} , respectively, i.e. the high-frequency band is definitely more affected. A good correlation between the wavenumber and the FWHM of the band was found (See Fig. S3 in the ESI). This indicates that temperature rise favours formation of H-bonds with negatively charged atoms from the framework (most probably oxygen atoms from the carboxylate groups). Unfortunately, there is no IR mode of this sample sensitive to the pore size, but the present results suggest that the position of the OH band could be used to monitor the phenomenon. In this respect we note that the 3721 cm^{-1} OH band of MIL-53(Al) (already associated with the large pore structure) is not present in the spectra of the NM sample. This is consistent with literature reports pointing out the very narrow pore form of the $\text{NH}_2\text{-MIL-53(Al)}$ material.^{20,28}

In summary, the hydroxyl groups in the MIL-53(Al) and $\text{NH}_2\text{-MIL-53(Al)}$ samples are involved in H-bonds with different strength and are monitored at different wavenumbers.

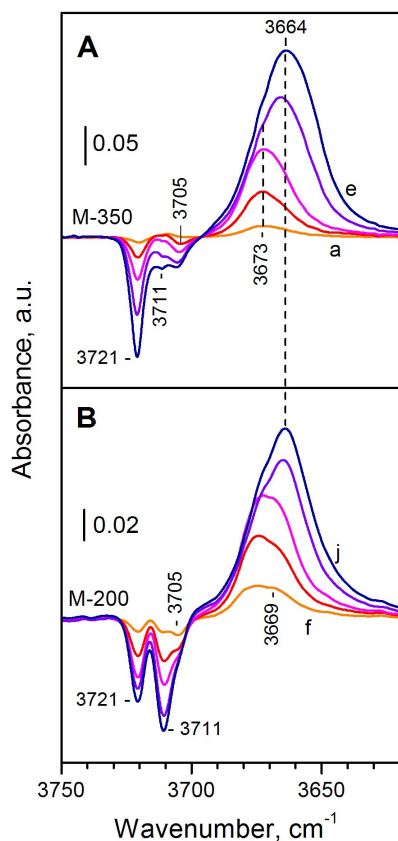


Fig. 4. Difference FTIR spectra of increasing amounts of CO adsorbed at low temperature on M-350 (panel A, spectra a-e) and M-200 (panel B, spectra f-j). The spectra are background corrected.

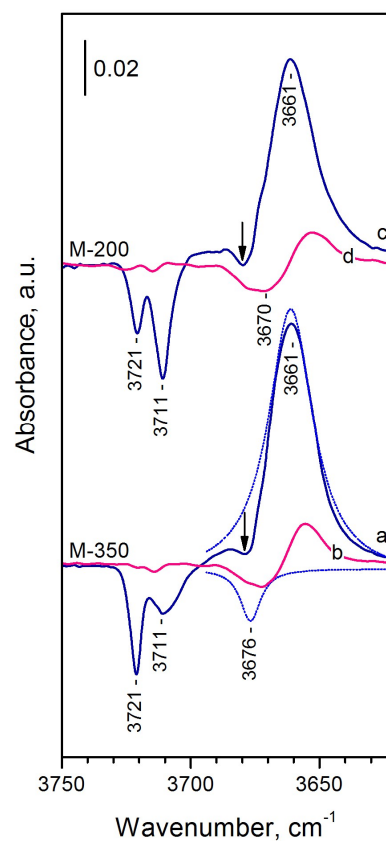


Fig. 5. Difference FTIR spectra of CO adsorbed at low temperature on M-350 (a, b) and M-200 (c, d). Spectra a and c represent differences between medium and low coverages and spectra b and d, differences between very high and high coverages.

Low-temperature adsorption of CO

Carbon monoxide is one of the most used probe molecules for determination of surface acidity.^{4,33} An important advantage of this molecule is that it is normally connected to the proton of the OH groups only by its C-atom and is adsorbed in end-on configuration. However, especially with porous materials, the possibilities of dual interaction should be considered.³¹ For convenience, some of the results obtained here using CO as a probe are summarized in Table 2.

Adsorption of CO on M-350. Fig. 4A presents the difference spectra registered after adsorption of CO at 100 K on the acid-free M-350 sample. Even at very low coverages two negative bands, at 3721 and 3705 cm^{-1} , are observed and a new band at 3673 cm^{-1} develops. The finding is in a general agreement with published data according to which the CO-induced shift of the OH modes of MIL-53(Al) is between -30 and -50 cm^{-1} .²¹ At slightly higher coverage, the weak component at 3711 cm^{-1} is also affected. Further increase of the CO coverage leads to additional erosion of the bands at

3721 and 3711 cm^{-1} and at the same time the maximum of the positive OH band is shifted to lower frequencies. Difference spectra (see Fig. 5A, spectrum a) clearly show a loss of a component at 3676 cm^{-1} (arrowed) and development of another band at 3661 cm^{-1} . We will use these values for further considerations because the spectra presented in Fig. 4A are due to superimposition of different bands.

Because the negative band at 3721 cm^{-1} is much more intense than the other negative bands, the observed phenomena can mainly be interpreted as two-stage interaction of the 3721 cm^{-1} OH groups with CO. This results in a shift of the band, first to 3676 cm^{-1} and then to 3661 cm^{-1} ($\Delta\nu_{\text{OH}}$ of -45 and -60 cm^{-1} , respectively). Therefore, we conclude that initially OH-CO adducts are formed and then are partly converted into geminal OH(CO)₂ species where the H-bond is bifurcated. A similar additional shift of $\nu(\text{OH})$ at high CO coverages has been reported with other materials and consensually assigned to solvation of the hydroxyl groups.⁴

To further confirm our conclusions we analyzed the spectra in the $\delta(\text{OH})$ and $\nu(\text{CO})$ regions. It is known that upon formation of H-bonds the $\delta(\text{OH})$ bands are shifted to higher frequencies.³⁴ Analysis of the negative $\delta(\text{OH})$ band is not utile because of the very high intensity of the original band (in such cases false features could be produced). However, the intensities of the shifted OH bands are much lower and therefore they can be followed. Fig. S4A in the ESI shows the shifted $\delta(\text{OH})$ band in presence of CO. Although the bands are complex and split because of the superimposition with (shifted) background bands, it appears that at low coverage the position of the shifted band is centred around 1020 cm^{-1} and at high coverages another complex band centred around 1035 cm^{-1} develops. Thus, the first and the second stage of the CO-induced shifts can be roughly estimated to be around -37 and -15 cm^{-1} , respectively. In the presence of CO in the gas phase practically no consumption of the original hydroxyls has been observed but conversion to geminal species takes place (see Fig. 5, spectrum b and Fig. S4, spectrum f, in the ESI). Note that in the presence of CO in the gas phase the $\nu(\text{OH})$ bands are gradually shifted to lower frequencies, which is most probably due to the cooperative effect of the CO molecules in the confined space. Details of the spectra in the carbonyl stretching region are provided in ESI (see Fig. S5).

A careful inspection of spectra a-c from Fig. 4A indicates a low-frequency shoulder(s) of the shifted OH band even at low CO coverage. These shoulders can be associated with the heterogeneity of the hydroxyls. However, it is impossible at this stage to draw definite conclusion about the shift of the bands at 3711 and 3705 cm^{-1} due to their low intensities.

Adsorption of CO on M-200. To obtain more information on the behaviour of the band at 3711 cm^{-1} we studied CO adsorption on the M-200 sample: it was already noted that this is the principal hydroxyl band with this material (see Fig. 3A, spectrum b).

Consider first the spectra at low-to-medium CO coverages (Fig. 4B, spectra f-h). Although the hydroxyl spectra of the sample are dominated by the band at 3711 cm^{-1} , two negative bands at 3721 and 3711 cm^{-1} of comparable intensities develop. This indicates a stronger interaction of the 3721 cm^{-1} hydroxyls with CO. In addition, weak negative band at 3705 cm^{-1} was registered even at low coverages. Consider now the positive bands. In addition to the feature at 3673 cm^{-1} (observed with the M-350 sample) a component at 3669 cm^{-1} is well discernible. Therefore, the band at 3711 cm^{-1} is shifted upon CO adsorption to 3669 cm^{-1} ($\Delta\nu(\text{OH}) = -42\text{ cm}^{-1}$). When

CO was present in the gas phase the perturbed OH band shifts to lower frequencies (see Fig. 4B, spectra i-j and Fig. 5, spectrum d). This indicates that the 3711 cm^{-1} band also interacts with CO at two stages. It is not possible to precisely determine the position of the shifted band because of the gradual shift occurring in presence of CO gas phase. However, taking into account the similarity of the spectra of the two samples at high coverage, we assume that the shifted band is around 3660 cm^{-1} . Thus, the two step interaction is characterized by $\Delta\nu(\text{OH})$ of -42 and ca. -50 cm^{-1} , respectively. In any case, the analysis of the $\delta(\text{OH})$ region indicates that the formation of bifurcated complexes is more hindered with this sample, likely due to the pore effect. Indeed, the overall intensity of the negative bands recorded with M-200 is lower as compared to the M-350 which is attributed to hindered access to the OH groups due to the presence of residual acid and the smaller pores of the material.

As for the weak band at 3705 cm^{-1} , again no clear information was observed from the experiments. We suggest that this low-intensity band is due either to impurities (possibly from extraframework alumina),³⁵ or to defects in the MOF framework.

Adsorption of CO on NM. Let consider now the amino-functionalized sample. The spectra recorded after CO adsorption on NM are shown in Fig. 6A. Three negative bands develop with increasing the CO coverage, their maxima being at 3711 , 3702 and 3683 cm^{-1} . At the same time a broad absorbance emerges and its maximum cannot be precisely determined because of the superimposition with the negative bands.

The band at 3702 cm^{-1} is of very low intensity and we cannot draw any definite conclusions about it. It seems that this band corresponds to the weak band at 3705 cm^{-1} found with the amino-free samples.

The interaction of the 3711 cm^{-1} band with CO on the M-200 sample leads, at low CO coverages, to the development of a band at 3669 cm^{-1} (see Fig. 4B). With the NM sample one can expect a similar interaction (the conclusions are supported by the $^{15}\text{N}_2$ adsorption experiments, see below). The spectra show an additional band with a maximum at 3661 cm^{-1} which is attributed to CO interaction with the 3683 cm^{-1} OH groups (Fig. 6A). The relatively low intensity is consistent with the small shift and the fact that the 3683 cm^{-1} band corresponds to hydroxyls that are already H-bonded.

With coverage increase the broad positive feature is shifted to lower wavenumbers which suggests formation of

Table 2. Spectral data for interaction of $^{15}\text{N}_2$ and CO with hydroxyl groups of the samples.

Sample	$\nu(\text{OH}),\text{ cm}^{-1}$	$\Delta\nu(\text{OH}),\text{ cm}^{-1}$ (medium $^{15}\text{N}_2$ coverage)	$\Delta\nu(\text{OH}),\text{ cm}^{-1}$ (medium CO coverage)	$\Delta\nu(\text{OH}),\text{ cm}^{-1}$ (high CO coverage)
M-350	3721-20	-12	-45	-60
M-200	3721-20	-12	-45	-60
	3711	-6	-42	-50
NM*	3711	-7	-39*	(-50)
	3683	0	-23	?

* the data are approximate because of the band superimposition.

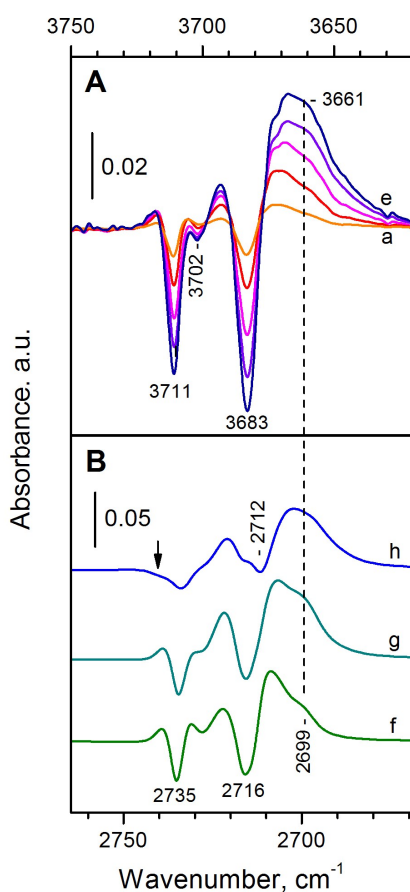


Fig. 6. Panel A: Development of the difference FTIR spectra registered after adsorption of increasing amounts of CO (up to 5 mbar equilibrium pressure) on NM sample. Panel B: Difference spectra reflecting small changes in the amount of adsorbed CO at low (f), medium (g) and high (h) CO coverages on deuterated self-supporting pellet of NM sample.

geminal complexes. These conclusions are supported by the spectra in the $\delta(\text{OH})$ region (Fig. S4C). A band at 1001 cm^{-1} (OH-CO adducts) is formed at low coverage. However, another band, at 1022 cm^{-1} develops even at medium coverages and is associated with the appearance of geminal species.

To follow more precisely these changes we studied CO interaction with deuterated self-supporting pellets. The spectra are presented in Fig. 6B where the X-axis scale is divided to the experimentally observed isotopic shift factor which allows direct comparison of the spectra in the OH and OD regions. A shoulder at 2699 cm^{-1} is clearly observed at low and medium CO coverages (Fig. 6B, spectra f, g) corresponding to a perturbed OH band at 3661 cm^{-1} . At high coverage (Fig. 6B, spectrum h) the formation of geminal species is well seen by the shift of the positive band to lower wavenumbers (note the arrowed negative feature corresponding to the highest-frequency components of the band).

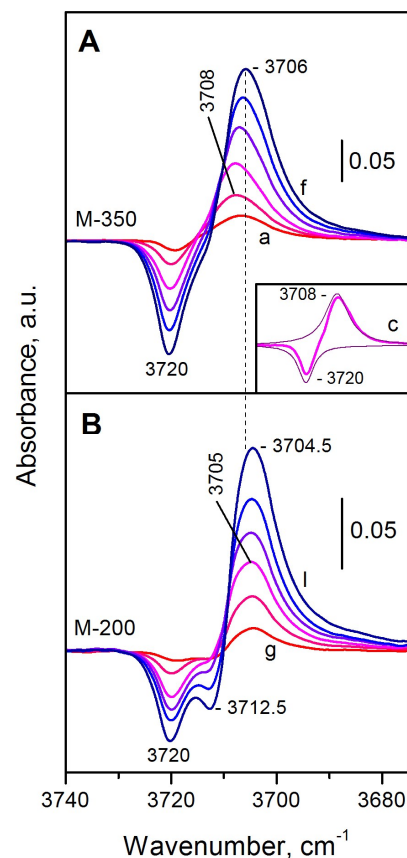


Fig. 7. Development of the difference FTIR spectra registered after adsorption of increasing amounts of $^{15}\text{N}_2$ (up to 50 mbar equilibrium pressure) at 100 K on the samples M-350 (panel A, spectra a-f) and M-200 (panel B, spectra g-l).

Low-temperature adsorption of $^{15}\text{N}_2$

Dinitrogen is another widely used molecular probe for measuring the acidity of OH groups.^{4,11,36-39} Important advantages of N_2 are that (i) this molecule is normally adsorbed in end-on configuration and (ii) the N-N modes in gas phase are IR inactive. We utilized the $^{15}\text{N}_2$ isotopologue in order to avoid any hindrance from the spectrum of CO_2 in the air. Note that it was reported that the basicity of $^{14}\text{N}_2$ and $^{15}\text{N}_2$ is practically the same.³⁶

Adsorption of $^{15}\text{N}_2$ on M-350. Fig. 7A presents the spectra in the hydroxyl region registered after contact of the M-350 sample with $^{15}\text{N}_2$ at 100 K. A shift of the OH band from 3720 to 3708 cm^{-1} is clearly observed at low-to-medium coverage ($\Delta\nu = -12\text{ cm}^{-1}$). Indeed, the spectra are well deconvoluted to these two bands. The results indicate a very weak acidity of the hydroxyls. For comparison, the N_2 -induced shift of $\nu(\text{OH})$ of the weakly acidic silanols on silica is -32 cm^{-1} .³⁷

At high coverage the shift is slightly larger (-14 cm^{-1}) which indicates initial stages of production of geminal complexes. This conclusion is supported by analysis of the low-frequency region where the $\delta(\text{OH})$ band is shifted to 1005 cm^{-1} , but at

high coverages a weak component at 1015 cm^{-1} also develops (spectra not shown). In any case, the process is much less pronounced as compared to the interaction of hydroxyls with CO. The ^{15}N - ^{15}N band of the complex is of very low intensity but was registered with self-supporting pellets at 2247.5 cm^{-1} . This value is close to the gas-phase Raman frequency and indicates a very weak interaction (for comparison the ^{15}N - ^{15}N stretching modes of $^{15}\text{N}_2$ complexes with bridging hydroxyls in H-ZSM-5 are observed at 2254 cm^{-1}).¹¹

Adsorption of $^{15}\text{N}_2$ on M-200. Due to the band superimposition, no clear conclusions about the acidity of the hydroxyls monitored at 3711 cm^{-1} can be drawn in this case. As in the case of CO adsorption, we have used for this purpose the M-200 sample (see Fig. 7B). It is seen that in this case the maximum of the shifted band is observed at slightly lower wavenumbers as compared to the M-350 sample. This suggests that the band at 3711 cm^{-1} is shifted to lower frequencies as compared to the band at 3720 cm^{-1} . It is also obvious that the band at 3720 cm^{-1} is preferentially affected at low $^{15}\text{N}_2$ coverages, while the lower-frequency band at high coverages. In attempt to determine more precisely the shift of the 3711 cm^{-1} band we deconvoluted series of difference spectra characterized by different intensity ratios of the two bands (Fig. S6 in the ESI). The results imply that when the low-frequency negative band dominates in the spectra the maximum of the shifted hydroxyl band is at 3705.5 cm^{-1} (Fig. S6, spectrum e). Taking into account the possible weak contribution of the higher frequency hydroxyls, we adopt the value of 3705 cm^{-1} for the shifted 3711 cm^{-1} band. Therefore, the $^{15}\text{N}_2$ induced shift in this case is ca. -6 cm^{-1} .

Finally, we note that the 3665 cm^{-1} OH groups (H-bonded to residual acid) are not affected by $^{15}\text{N}_2$ adsorption.

Adsorption of $^{15}\text{N}_2$ on NM. Let consider now the NM sample (Fig. 8). The difference spectra show that the band at 3711 cm^{-1} is shifted upon $^{15}\text{N}_2$ adsorption to 3704 cm^{-1} (see the inset in Fig. 8A) which is similar to the observations made with the M-200 sample. In addition, the band at 3683 cm^{-1} is also affected. Looking at the spectra presented in panel A, one might conclude that the band is shifted to 3676 cm^{-1} , which corresponds to a $\Delta\nu(\text{OH})$ of ca. -7 cm^{-1} . However, inspection of the original spectra (registered with deuterated sample) indicates that this is not the case (see Fig. 8B). While the higher-frequency band at 2735 cm^{-1} (corresponding OH band at 3711 cm^{-1}) is indeed shifted, the band at 2715 cm^{-1} (corresponding OH band at 3683 cm^{-1}) is rather broadened. This reflects in the appearance of one negative and two positive bands in the difference spectra.

Discussion

A general picture that arises from our results is that, with all samples and at identical conditions, the fraction of hydroxyls affected by CO is larger than the fraction affected by $^{15}\text{N}_2$. Taking into account the similar critical and kinetic diameters of the two adsorbate molecules,⁴ the phenomenon should be related to the higher basicity of CO as compared to $^{15}\text{N}_2$. Also, with the M-350 sample the amount of OH groups interacting

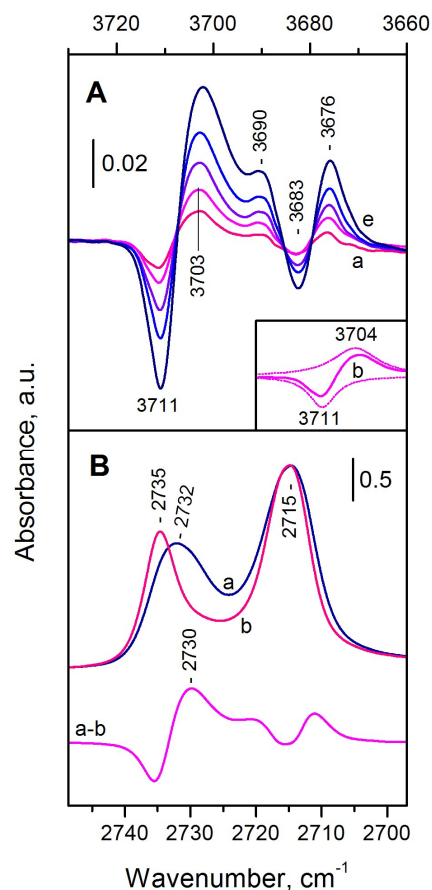


Fig. 8. Panel A: Development of the difference FTIR spectra registered after adsorption of increasing amounts of $^{15}\text{N}_2$ (up to 50 mbar equilibrium pressure) at 100 K on the NM sample. The inset shows computer deconvolution of spectrum "b" on the $3725 - 3705\text{ cm}^{-1}$ region. Panel B: FTIR spectra registered after adsorption of $^{15}\text{N}_2$ at 100 K on deuterated self-supporting pellet of NM (a) and after short evacuation at 100 K (b).

with probe molecules is larger than with the other samples. One of the reasons for this is the easy access of guest molecules related to the large pore structure of this material. The effect of different factors on the pore structure of MIL-53 samples has recently been reviewed²⁸ and it was noted that the difference in the energy of narrow and large pore forms of MIL-53(Al) is very small. In contrast, the framework of NH_2 -MIL-53(Al) is stable in the narrow pore form which hinders the adsorption of CO and N_2 .

There are huge amounts of data describing the CO- and N_2 -induced shift of the OH stretching modes of various hydroxyls. It is well established that the CO-induced shift is ca. 2.7 times larger than the N_2 -induced one.^{4,11,38} However, the precision of the H-bond method for measuring acidity of OH groups have been questioned.⁸ We believe that the present results could explain some reported deviations from the theory. Fig. 9 (the circles) presents a plot of CO-induced vs. $^{15}\text{N}_2$ -induced shifts of

the OH modes with our samples. The dotted line corresponds to the correlation established on the basis of literature data concerning more acidic hydroxyls.⁴

We are going to discuss first the hydroxyl band at 3683 cm^{-1} recorded with the NM sample. It is shifted after adsorption of CO but not by $^{15}\text{N}_2$ adsorption. This fact is easy to explain taking into account that the strength of the H-bond formed between the structural OH groups and amino groups is intermediate between the strength of the H-bond formed with CO and $^{15}\text{N}_2$. Indeed, taking as a reference the hydroxyl band at 3721 cm^{-1} , it is shifted after interaction with $^{15}\text{N}_2$, amino groups and CO, by -12, -38 and -45 cm^{-1} respectively. Therefore, replacement of the amino-groups as a ligand by CO will be energetically favored (see Fig. 10a) while $^{15}\text{N}_2$ is too weak base to do this (Fig. 10b).

The idea of breaking the pre-existing H-bonds when hydroxyl groups form adducts with probe molecules is not new. Nachtigall et al.⁸ pointed out that when the Brønsted-acid OH group is preliminary involved in H-bonding the CO adsorption enthalpy should be lower, because the hydrogen atom must move to a position from where it can efficiently interact with the adsorbate.

Very recently similar conclusions have been made as a result of investigations of MIL-53(Fe)-X (X = Cl, Br).^{26,31} Two types of OH groups were observed by IR spectroscopy with these samples: (i) free hydroxyls and (ii) OH groups that were involved in H-bonding with halogen atoms. Adsorption of CO_2 led to the appearance of only one perturbed band suggesting the same interaction with the two families of hydroxyls and breaking the pre-existing H-bond.²⁶ The same conclusions were made after adsorption of propyne.³¹

Let now discuss the hydroxyl bands at 3721 and 3711 cm^{-1} . Both bands are shifted after adsorption of CO and $^{15}\text{N}_2$ and, as expected, the CO induced shift is larger. However, there are serious deviations from the expected results (the dashed line in Fig. 9). For instance, based on the CO induced shift (-45 cm^{-1}), the band at 3721 cm^{-1} should be shifted by -16.5 cm^{-1} after adsorption of $^{15}\text{N}_2$. Similar is the situation with the band at 3711 cm^{-1} and these phenomena need explanation.

Table 3 presents the calculated PAs of the 3721 and 3711 cm^{-1} hydroxyl groups using the data obtained after CO and $^{15}\text{N}_2$ adsorption and acc. to equation 1. It is seen that the two probes give different values and the difference are very important with the 3711 cm^{-1} hydroxyls. Evidently, the reasons are associated with the fact that the hydroxyls on the activated samples are already H-bonded. Indeed, the effects decrease with the decrease of the strength of the pre-existing H-bond.

Gil et al.¹³ noted that the lower value of the CO induced shift of H-bonded hydroxyls cannot be interpreted in terms of a lower acidity because this is only an additional frequency downshift. Note that hydroxyl groups in porous materials are normally involved in weak H-bonding with the framework. Our results indicate that even the hydroxyls monitored by the band at 3721 cm^{-1} also participate in H-bonding, although weak.

Let us assume that after adsorption of CO or $^{15}\text{N}_2$ the pre-existing H-bond is totally broken (Fig. 10, scheme a). Simple calculations (see ESI, Section 8) show that, if the intrinsic

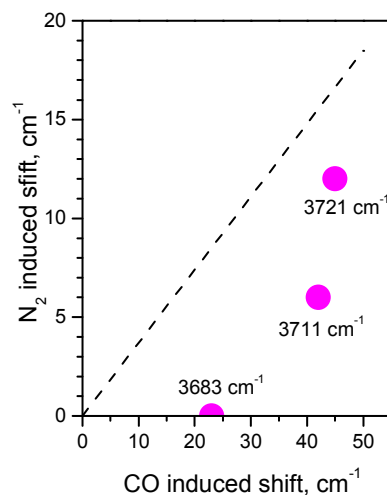


Fig. 9. Plot of CO- vs. $^{15}\text{N}_2$ -induced shift of OH stretching modes. The dashed line corresponds to a correlation established on the basis of literature data. Band at 3721 cm^{-1} registered with M-350 sample; band at 3711 cm^{-1} registered with M-200 sample; and band at 3683 cm^{-1} registered with NM sample.

frequency of the free structural hydroxyls is 3727 cm^{-1} , the CO induced shift (taking 3727 cm^{-1} as a reference value) will be -51 cm^{-1} , and the $^{15}\text{N}_2$ induced shift, -18 cm^{-1} . The ratio between these two values is 2.8, as the ratio measured for silanol groups. Practically the same ratio is obtained taking into account the measured CO- and $^{15}\text{N}_2$ -induced shifts of the band at 3711 cm^{-1} . Moreover, the calculated PAs using the data with the two probes almost coincide (see Table 3). Thus, the experimental deviations find a simple explanation. Note that this approach appears to be very useful to estimate the intrinsic frequency of hydroxyls in various porous materials.

Table 3. PA of OH groups in MIL-53(Al) measured by the H-bond method.

OH group	CO adsorption	$^{15}\text{N}_2$ adsorption
	Measured PA	
3721 cm^{-1}	1523 kJ mol^{-1}	1578 kJ mol^{-1}
3711 cm^{-1}	1536 kJ mol^{-1}	1712 kJ mol^{-1}
PA after correction using $\nu(\text{OH})$ at 3727 cm^{-1} as a reference		
3721 cm^{-1}	1499 kJ mol^{-1}	1501 kJ mol^{-1}
3711 cm^{-1}	1475 kJ mol^{-1}	1462 kJ mol^{-1}

Although the above approach explains to a large extent the observed deviations, analysis of the spectra indicates that the real situation is more complicated. Indeed, based only on the Scheme 1a (Fig. 10), one should expect the 3711 cm^{-1} band to be shifted after adsorption of a guest molecule to the same wavenumbers as the band at 3721 cm^{-1} . However, it was observed that the shift is slightly larger. This observation can be explained by the formation of complexes with bifurcated H-bonds (Scheme 1b in Fig. 10).

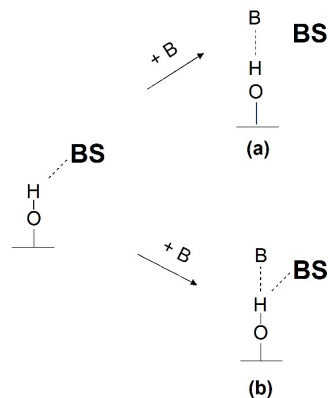


Fig. 10. Schematic presentation of two possible ways of interaction of basic probe molecules with hydroxyl groups involved in H-bonding with the framework of porous materials. **BS** denotes a basic site from the framework and **B**, a basic guest molecule.

Let now consider first the formation of bifurcated complexes with two equal bases. This is exemplified by the geminal carbonyl species. Using the wavenumber of 3727 cm^{-1} as a reference OH value, it appears that the real CO induced shift of the OH modes in the formation of OH-CO adducts is -51 cm^{-1} (at this stage the eventual interaction of the proton from the adduct with the MOF framework will be neglected). Formation of an H-bond with a second CO molecule leads to additional shift of $\nu(\text{OH})$ by -15 cm^{-1} . Therefore, the cooperative action of two identical bases when bifurcated H-bond is formed leads to an additional shift of the OH modes which is, however, smaller than the shift caused by the interaction with one basic molecule.

When CO or N_2 interact with the 3721 or 3711 cm^{-1} OH groups to form 1 : 1 complexes, the proton remains still bonded to the framework site although the bond is weakened. This reflects in a slight increase of the $\nu(\text{OH})$ shift values. The effect is more pronounced with the band at 3711 cm^{-1} and results in a slight overestimation of the acidity of these hydroxyls (see Table 3, corrected values). The residual H-bond with the framework is weak when carbonyls are formed and practically broken when geminal carbonyls are produced. As a result, in the latter case the two bands (at 3721 and 3711 cm^{-1}) are practically shifted to the same position. It is not possible to conclude from our results whether geminal dicarbonyls are formed with the OH-CO adduct produced with the 3683 cm^{-1} hydroxyls because they should be spectrally observed very near to the bifurcated complexes having one CO ligand. It seems likely that the two forms are in equilibrium.

Our results show that the effect of the bifurcated H-bond is particularly important when the strength of the two bonds is comparable. With increasing the basicity of the probe molecule the effect fades. It should also decrease with increasing the acidity of the hydroxyls which explains the good reported correlation found in the literature between the CO-

and N_2 -induced shifts of $\nu(\text{OH})$ modes. Indeed, the reported data concerns mainly "free" hydroxyls (SiO_2) or strongly acidic hydroxyls (bridging OHs in zeolites). However, with weakly acidic and H-bonded hydroxyls, as in MOF samples, the effects are important and should be considered.

In summary, the preliminary H-bonding has an important effect on the adsorbate-induced shift of the OH stretching modes. The measured shift is only additional: it should correlate with the enthalpy of adsorption but is not indicative of the acidity of hydroxyls. To measure the PA it is necessary to use the intrinsic frequency of the OH groups as a reference value. Formation of bifurcated H-bond leads to a slight overestimation of the PA.

Conclusions

Two hydroxyl bands, at 3721 and 3711 cm^{-1} , respectively, are registered with the MIL-53(Al) MOF sample at 100 K. This heterogeneity is attributed to the coexistence of the "large pore" and "narrow pore" forms of the MOF structure. All hydroxyls are H-bonded to the MOF framework but the strength of the H-bond is higher for the 3711 cm^{-1} hydroxyls (associated with the "narrow pore" form).

The OH groups in NH_2 -MIL-53(Al) MOF sample are also of two types (IR bands at 3711 and 3683 cm^{-1} , respectively, at 100 K). The 3711 cm^{-1} OH groups are analogues to the "narrow pore" hydroxyls of the amino-free sample. The OH groups monitored at 3683 cm^{-1} are involved in H-bonding with the amino groups.

All hydroxyls in MIL-53(Al) and NH_2 -MIL-53(Al) MOF samples are characterized by weak acidity. Guest molecules (CO, $^{15}\text{N}_2$) do not interact with hydroxyls which are already involved in strong H-bonding with the MOF framework (stronger than the hydrogen bond expected to be formed with the adsorbate).

Depending on the strength of interaction, the adsorption of a guest molecule can lead to breaking or weakening of the pre-existing H-bond. In the latter case bifurcated complexes are formed.

Comparing the CO- and N_2 -induced shift of the OH modes allows estimating the intrinsic frequency of the OH groups (i.e. if they are not involved in any H-bonding). The use of this frequency as a reference value allows a precise determination of the hydroxyl acidity by the hydrogen-bond method.

Acknowledgements

The research leading to these results has received funding from the European Union Seventh Framework Programme (FP7/2007-2013) under grant agreement n° 608490, project M4CO2. The authors thank Prof. F. Kapteijn and Prof. J. Gascon (TU Delft) for providing the NH_2 -MIL-53(Al) sample and Prof. M. Daturi for some helpful discussion.

Notes and references

- G. Busca, *Chem. Rev.* 2007, **107**, 5366–5410.
- E. G. Derouane, J. C. Védrine, R. Ramos Pinto, P. M. Borges, L. Costa, M. A. N. D. A. Lemos, F. Lemos and F. Ramôa Ribeiro, *Catal. Rev. Sci. Eng.* 2013, **55**, 454–515.
- H. G. Karge and E. Geidel, *Mol. Sieves* 2004, **4**, 1–200.
- K. Hadjiivanov, *Adv. Catal.* 2014, **57**, 97–318.
- F. Thibault-Starzyk and F. Maugé, in *Characterization of Solid Materials and Heterogeneous Catalysts. From Structure to Surface Reactivity* (M. Che and J. C. Védrine, Eds.), Wiley, VCH, Weinheim, 2012, Vol. 1, pp. 3–48.
- E. A. Paukshtis and E. N. Yurchenko, *Russ. Chem. Rev.* 1983, **52**, 242–258.
- E. P. L. Hunter and S. G. Lias, *J. Phys. Chem. Ref. Data* 1998, **27**, 413–656.
- C. O. Arean, M. R. Delgado, P. Nachtigall, H. V Thang, M. Rubes, R. Bulánek and P. Chlubná-Eliášová, *Phys. Chem. Chem. Phys.* 2014, **16**, 10129–10141.
- H. Knözinger and S. Huber, *J. Chem. Soc. Faraday Trans.* 1998, **94**, 2047–2059.
- S. Kotrel, J. H. Lunsford and H. Knözinger, *J. Phys. Chem. B* 2001, **105**, 3917–3921.
- K. Chakarova and K. Hadjiivanov, *Chem. Commun.* 2011, **47**, 1878–1880.
- P. A. Jacobs and W. J. Mortier, *Zeolites* 1982, **2**, 226–230.
- B. Gil, G. Košová and J. Čejka, *Microporous Mesoporous Mater.* 2010, **129**, 256–266.
- L. Dimitrov, M. Mihaylov, K. Hadjiivanov and V. Mavrodinova, *Microporous Mesoporous Mater.* 2011, **143**, 291–301.
- M. Trombetta, G. Busca, S. Rossini, V. Piccoli, U. Cornaro, A. Guercio, R. Catani and R. J. Willey, *J. Catal.* 1998, **179**, 581–596.
- M. Bevilacqua, T. Montanari, E. Finocchio and G. Busca, *Catal. Today* 2006, **116**, 132–142.
- W. Daniell, U. Schubert, R. Glöckler, A. Meyer, K. Noweck and H. Knözinger, *Appl. Catal. A* 2000, **196**, 247–260.
- G. Crépeau, V. Montouillout, A. Vimont, L. Mariey, T. Cseri and F. Mauge, *J. Phys. Chem. B* 2006, **110**, 15172–15185.
- J. Gascon, U. Aktay, M. D. Hernandez-Alonso, G. P. M. van Klink and F. Kapteijn, *J. Catal.* 2009, **261**, 75–87.
- P. Serra-Crespo, E. Gobechiya, E. V. Ramos-Fernandez, J. Juan-Alcañiz, A. Martinez-Joaristi, E. Stavitski, C. E. A. Kirschhock, J. A. Martens, F. Kapteijn and J. Gascon, *Langmuir* 2012, **28**, 12916–12922.
- U. Ravon, G. Chaplais, C. Chizallet, B. Seyyedi, F. Bonino, S. Bordiga, N. Bats and D. Farrusseng, *ChemCatChem* 2010, **2**, 1235–1238.
- C. Volkringer, T. Loiseau, N. Guillou, G. Férey, E. Elkaim, A. Vimont, *Dalton Trans.* 2009, **38**, 2241–2249.
- B. Zornoza, A. Martinez-Joaristi, P. Serra-Crespo, C. Tellez, J. Coronas, J. Gascon and F. Kapteijn, *Chem. Commun.* 2011, **47**, 9522–9524.
- A. Vimont, A. Travert, P. Bazin, J.-C. Lavalley, M. Daturi, C. Serre, G. Férey, S. Bourrelly and P. L. Llewellyn, *Chem. Commun.* 2007, **43**, 3291–3293.
- B. Seoane, C. Téllez, J. Coronas and C. Staudt, *Separation Purification Technol.* 2013, **111**, 72–81.
- T. Devic, F. Salles, S. Bourrelly, B. Moulin, G. Maurin, P. Horcajada, C. Serre, A. Vimont, J.-C. Lavalley, H. Leclerc, G. Clet, M. Daturi, P. L. Llewellyn, Y. Filinchuk and G. Férey, *J. Mater. Chem.* 2012, **22**, 10266–10273.
- M. Valero, B. Zornoza, C. Téllez and J. Coronas, *Microporous Mesoporous Mater.* 2014, **192**, 23–28.
- E. Stavitski, E. A. Pidko, S. Couck, T. Remy, E. J. M. Hensen, B. M. Weckhuysen, J. Denayer, J. Gascon and F. Kapteijn, *Langmuir* 2011, **27**, 3970–3976.
- T. Rodenas, M. van Dalen, P. Serra-Crespo, F. Kapteijn, J. Gascon, *Microporous Mesoporous Mater.* 2014, **192**, 35–42.
- T. Rodenas, M. van Dalen, E. García-Pérez, P. Serra-Crespo, B. Zornoza, F. Kapteijn and J. Gascon, *Adv. Funct. Mater.* 2014, **24**, 249–256.
- B. Moulin, F. Salles, S. Bourrelly, P. L. Llewellyn, T. Devic, P. Horcajada, C. Serre, G. Clet, J.-C. Lavalley, M. Daturi, G. Maurin and A. Vimont, *Microporous Mesoporous Mater.* 2014, **195**, 197–204.
- F. Ragon, B. Campo, Q. Yang, C. Martineau, A. D. Wiersum, A. Lago, V. Guillerme, C. Hemsley, J. F. Eubank, M. Vishnuvarthan, F. Taulelle, P. Horcajada, A. Vimont, P. L. Llewellyn, M. Daturi, S. Devautour-Vinot, G. Maurin, C. Serre, T. Devic and G. Clet, *J. Mater. Chem. A* 2015, **3**, 3294–3309.
- K. Hadjiivanov and G. Vayssilov, *Adv. Catal.* 2002, **47**, 307–511.
- C. Paze, S. Bordiga, C. Lamberti, M. Salvalaggio, A. Zecchina and G. Bellussi, *J. Phys. Chem. B* 1997, **101**, 4740–4751.
- G. Busca, *Adv. Catal.* 2014, **57**, 319–404.
- K. M. Neyman, P. Strodel, S. P. Ruzankin, N. Schlenso, H. Knözinger and N. Rösch, *Catal. Lett.* 1995, **31**, 273–285.
- K. Chakarova, N. Drenchev, M. Mihaylov, P. Nikolov and K. Hadjiivanov, *J. Phys. Chem. C* 2013, **117**, 5242–5248.
- F. Wakabayashi, J. Kondo, K. Domen and C. Hirose, *J. Phys. Chem.* 1995, **99**, 10573–10580.
- F. Wakabayashi and K. Domen, *Catal. Surv. Jpn.* 1997, **1**, 181–193.

